Analysis of the ferroelastic phase transition of $N(CH_3)_4MnCl_3$ (TMMC) by means of x-ray diffraction study

1997 J. Phys.: Condens. Matter 9 937

(http://iopscience.iop.org/0953-8984/9/4/013)

J. Phys.: Condens. Matter **9** (1997) 937–949. Printed in the UK PII: S0953-8984(97)76036-3

Analysis of the ferroelastic phase transition of $N(CH_3)_4MnCl_3$ (TMMC) by means of x-ray diffraction study

G Aguirre-Zamalloa†, V Rodriguez†, M Couzi†, F Sayetat‡ and P Fertey‡

† Laboratoire de Spectroscopie Moléculaire et Cristalline (URA 124 CNRS), 351 cours de la Libération, Université de Bordeaux I, F-33405 Talence Cédex, France

‡ Laboratoire de Cristallographie, CNRS, 166X, F-38042 Grenoble Cédex, France

Received 8 July 1996

Abstract. The order–disorder phase transition in the linear chain compound $N(CH_3)_4MnCl_3$ (TMMC) was investigated by means of x-ray diffraction. The hexagonal structure at room temperature (space group $P6_3/m$ with $Z = 2$) is characterized by an orientational disorder of the organic group TMA. A weakly first-order phase transition occurs at 126 K which stabilizes a monoclinic low-temperature phase (space group $P2_1/b$ with $Z = 4$) characterized by a doubling of the hexagonal unit cell along the b direction. The cell parameters were determined in a large range of temperature including the two phases (from 5 to 300 K) and the extent of lattice distortion was measured in the ordered monoclinic phase. The temperature dependences of both the spontaneous strain component ($e_1 - e_2$) and the intensity of superstructure reflections were analysed by a Landau type free energy expansion involving two coupled order parameters necessary to account for this 'triggered' phase transition.

1. Introduction

Tetramethylammonium manganese (II) chloride, $N(CH_3)_4MnCl_3$ (TMMC), exhibits a one-dimensional type structure, built up from infinite chains made of $MnCl_6$ octahedra sharing opposite faces. The space between chains is occupied by the $[N(CH_3)_4]^+$ cations (TMA) [1]. At ambient pressure, TMMC undergoes at 126 K a weakly first-order structural phase transition from a disordered hexagonal phase (phase I) with space group $P6_3/m$ and $Z = 2$ formula units per unit cell to an ordered monoclinic phase (phase II) [2]. This phase transition is governed essentially by the reorientational dynamics of the TMA groups [2–10].

The space group and structure of the monoclinic low-temperature phase have been the subject of numerous discussions [2–9]. At present, it is confidently established that the space group is $P2_1/b$ with $Z = 4$ [10] (unique axis along $\boldsymbol{c}$), Thus corresponding to a doubling of the hexagonal unit cell along the $\boldsymbol{b}$ axis. In such a situation, point M ($0\ \frac{1}{2}\ 0$) at the hexagonal Brillouin zone boundary [11] is replaced at zone centre in phase II. The orientational disorder of the TMA groups in phase I was appropriately described in terms of a complex Frenkel type six-site model, in which the TMAs occupy instantaneously the general position [10]. Moreover, the 'frozen' orientation of the TMA found in the ordered phase II practically coincides with one out of the six energetically equivalent orientations in the hexagonal phase. The I $\leftrightarrow$ II transition is further characterized by an antiphase translational displacement of the octahedra chains along the hexagonal axis, as a result of the freezing

0953-8984/97/040937+13$19.50

of the transverse acoustic mode TA(M) at point M, coupled with the orientational ordering process of the TMA groups [7, 9, 10].

The I $\leftrightarrow$ II phase transition of TMMC is ferroelastic since it involves the change of the crystalline system from hexagonal to monoclinic. Ultrasonic measurements [12] have shown a marked softening of the C_{66} elastic constant in the hexagonal phase when the transition temperature $T_c = 126$ K is approached from above. This observation strongly speaks in favour of a proper (or pseudo-proper) ferroelastic transition, despite the existence of cell doubling, which usually would characterize an improper ferroelastic. Hence, in the frame of Landau theory, a phenomenological thermodynamic potential has been proposed [13] in which η, a zone centre order parameter (OP) with E_{2g} symmetry, is bi-linearly coupled with the $(e_1 - e_2)$ and e_6 components of the strain tensor, to account for the softening of C_{66}. Furthermore, in order to achieve the observed unit-cell doubling, η 'triggers' a zone-boundary OP denoted as ξ, with M_1^-/A_u symmetry (according to the notations of Bradley and Cracknell [11]), through coupling terms of the form $\eta\xi^2$. It is worth noting that such a potential also predicts the existence of another monoclinic phase with space group $P2_1/m$ and $Z = 2$ (phase III), corresponding to the solution $\eta \neq 0$, $\xi = 0$. This phase III of TMMC can be stabilized under hydrostatic pressure above 0.2 GPa, [2, 8, 14]. However, it should be remarked that the only pertinent experimental evidence (other than symmetry considerations) upon which this model was actually established is the behaviour of the C_{66} elastic constant [12, 13]. To date, no systematic measurement of the coupled OPs η and ξ that drive the phase transition has been performed. Therefore, it is necessary to assemble other experimental data to confirm (or eventually deny) the validity of this model on more serious grounds.

In this work, we report powder x-ray diffraction measurements of TMMC carried out in a large range of temperature aiming at (i) the determination of the thermal evolution of the components of the spontaneous strain tensor which are associated with the OP η and (ii) the measurement of the temperature dependence of the superstructure reflections observed in the monoclinic phase, related to the OP ξ. Then, these results will be compared with predicted behaviours according to the model mentioned above [13].

2. Experimental details

Rapid evaporation at 333 K of saturated acidic aqueous solution containing stoichiometric amounts of $N(CH_3)_4Cl$ and $MnCl_2$ (Merck) yields small pink crystalline samples of TMMC. These were finally ground and sieved to obtain a homogeneous powder.

A powder x-ray counter diffractometer with Seeman–Bohlin setting has been used, with monochromatized chromium $K\alpha_1$ radiation ($\lambda = 2.289\,62$ Å), working in the 3–470 K temperature range [15]. The choice of this long-wavelength radiation provides us with a good resolution: this is particularly interesting for the study of the monoclinic phase of TMMC which presents a large lattice parameter ($b \approx 18$ Å) and consequently reflections very closely spaced on the powder diffraction pattern. Measurements have been limited to the domain of $48^\circ < 2\theta < 72^\circ$ by steps of 0.02° in 2θ. This choice represents a reasonable compromise between the resolution and overlapping of diffraction peaks at large angles. Note also that the intensity of reflections affected by strong Debye–Waller factors, particularly in the disordered phase [10], fades away exponentially as the scattering angle increases. The counting time was set to 40 s/point to guarantee an acceptable statistic, with a typical generator power of about 30 kW.

The data have been fitted by means of pattern matching refinement, which is a standard option in the extended Rietveld refinement program FULLPROF [16]. This treatment

consisted in fitting the while diffraction pattern using a profile model with arbitrary structure factor calculations. The fitted parameters are the cell parameters, a constant background intensity and the angular offset. The profile parameters were optimized and set constant during the refinement process.

3. Results

The diffraction patterns recorded in the temperature range of 20 K $< T <$ 300 K are shown in figure 1. Two selected diffraction patterns corresponding one to the hexagonal and one to the monoclinic phase are represented in figure 2. The phase transition is clearly evidenced by the splitting of diffraction peaks due to the change of the crystal class from $6/m$ to $2/m$, and by the appearance of superstructure reflections due to the doubling of the unit cell along the $\boldsymbol{b}$ axis. Some of the most apparent superstructure reflections are indicated in figure 2.

Besides, the temperature dependences of the lattice parameters extracted from the pattern matching refinements are reported in figure 3. In the monoclinic phase, $b_m/2$ was plotted for a direct comparison with the $a_h = b_h$ parameter of the hexagonal phase. The linear extrapolations, that can reasonably be performed in the low-temperature phase from the data in the high-temperature phase, are also shown in this figure: they represent 'baselines' which take into account the thermal expansion of the crystal and so permit us to calculate the excess contribution from the phase transition [17]. It is worth noting that our results in the monoclinic phase, concerning the a and b lattice constants, differ rather from those previously reported by Peercy *et al* using single-crystal photographic methods [2], but look more similar to those of Hutchings *et al* obtained by means of neutron diffraction [3]. These discrepancies might originate from the complex twinning that always occurs in the low-temperature phase [2, 3, 9]. Since in powder diffraction measurements twinning problems no longer exist, our results should be more relevant ones.

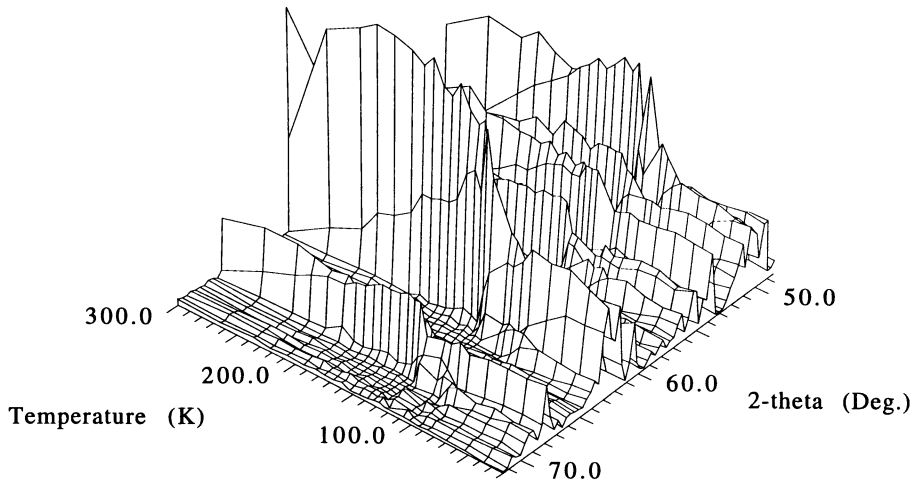

Figure 1. X-ray diffraction patterns of TMMC recorded at different temperatures ranging from 20 to 300 K at wavelength $\lambda = 2.289\,62$ Å.

From these data, the strain tensor components (i.e. $(e_1 - e_2)$ and e_6 with E_{2g} symmetry in the hexagonal phase), that yield spontaneous strains in the monoclinic phase, can easily

be calculated from the relations [17, 18]

$$e_1 - e_2 = (2a \sin\gamma - \sqrt{3}b)/\sqrt{3}a_0$$
$$e_6 = (2a \cos\gamma + b)/\sqrt{3}a_0$$

where a_0 is the temperature dependent extrapolated value of a_h (see figure 3) and $b = b_m/2$, as mentioned already. The temperature dependences of $(e_1 - e_2)$ and e_6 are reported in figure 4. It is clearly seen that the e_6 component is much smaller than $(e_1 - e_2)$. In fact, e_6 remains very weak because of a subtle balance between the thermal variations of the lattice parameters $\boldsymbol{a}$, $\boldsymbol{b}$ and γ. The $(e_1 - e_2)$ component takes relatively large values at low temperatures; in the following section, we intend to analyse its thermal evolution to ascertain whether or not it matches the behaviour predicted by the proposed Landau effective potential [13].

Finally, the thermal evolutions of the structure factors of superstructure reflections (which appear in the monoclinic phase) have been extracted from the pattern matching refinements and their intensities I_s. These reflections are related to the doubling of the unit cell at point M (0 $\frac{1}{2}$ 0) of the hexagonal Brillouin zone and so give a measure of the OP ξ. More precisely, since the static atomic displacements occurring through the phase transition of TMMC are small [9, 10], $I_s \propto \xi^2$ [19]. The superstructure reflection with Miller indices $(2\bar{5}2)$, which is fairly well isolated on the present diffraction patterns of the monoclinic phase (figure 2), has been selected. The plot of I_s (2 $\bar{5}$ 2) as a function of $(e_1 - e_2)$ is represented in figure 5: a good proportionality relation is observed. This point will be detailed in the following section.

4. Discussion

4.1. Definition of the order parameters

Let us recall briefly the physical sense of the primary OP η at zone centre and that of the 'triggered' one, ξ, at the zone-boundary point M, which were introduced in the proposed free energy expansion [13]. It has been clearly established that η is solely related to the disorder processes of the TMA [12], which were depicted successfully in the frame of a six-site Frenkel (jump) model [10, 20]. From such models, pseudo-spin coordinates expressed in terms of occupation probabilities of the TMA in their different possible orientations can be derived: they act as order parameters responsible for the phase transition [12, 13, 21]. The actual pseudo-spin coordinates related to the six-site model will not be reported here since a basically equivalent group-theoretical analysis has already been developed in full detail for the parent crystal $N(CH_3)_4CdBr_3$ (TMCB) [21]. Let us however indicate the symmetry properties of these pseudo-spin variables at zone centre:

$$R(\Gamma) = B_g + E_{1g} + E_{2g} + A_u + E_{1u} + E_{2u}$$

and at the M point

$$R(M) = 2M_1^+/A_g + 3M_2^+/B_g + 3M_1^-/A_u + 2M_2^-/B_u.$$

The analysis of these coordinates implies necessary conditions to reach a completely ordered ground state [21]. In the case of the monoclinic phase, with space group $P2_1/b$ ($Z = 4$), it can be shown that the achievement of the experimentally observed ordered state [10] requires the simultaneous 'freezing' of one pseudo-spin variable at zone centre with E_{2g} symmetry (thus corresponding to η) and of two coordinates at point M (0 $\frac{1}{2}$ 0), with M_1^-/A_u symmetry (thus corresponding to ξ). Let us point out that ξ also contains

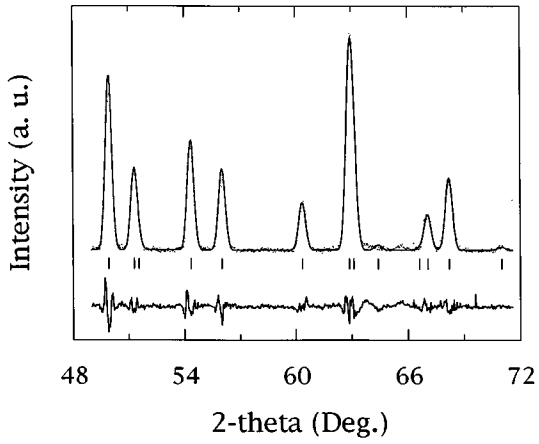

(*a*)

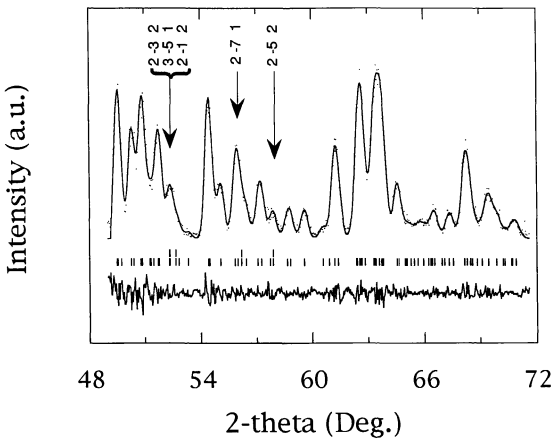

(*b*)

Figure 2. X-ray diffraction patterns of TMMC recorded (*a*) in the hexagonal phase at 130 K and (*b*) in the monoclinic phase at 20 K ($\lambda = 2.289\,62$ Å). The observed profiles are shown as dots and the calculated profiles as smooth curves; short vertical markers represent reflections allowed by symmetry. Difference profiles are represented at the bottom of the figures.

a displacive contribution due to the transverse acoustic mode TA(M) [9, 10] coupled with the relevant pseudo-spin coordinate (M_1^-/A_u symmetry) attached to the reorientations of the TMA groups [7]. In spite of the complex nature of the OP ξ, we are bound in this first analysis to consider ξ as a whole, since the superlattice reflections include both order–disorder and displacive contributions.

4.2. The Landau free energy expansion

As proposed in a previous study [13], the Landau free-energy expansion that accounts for the 'triggered' I $\leftrightarrow$ II phase transition can be written

$$\Delta\Phi(\eta, e, \xi) = \Delta\Phi(\eta) + \Delta\Phi(e) + \Delta\Phi(\eta, e) + \Delta\Phi(\xi) + \Delta\Phi(\eta, \xi). \qquad (1)$$

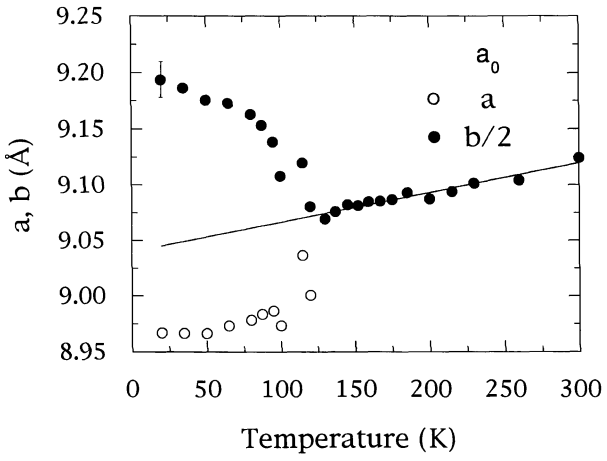

(*a*)

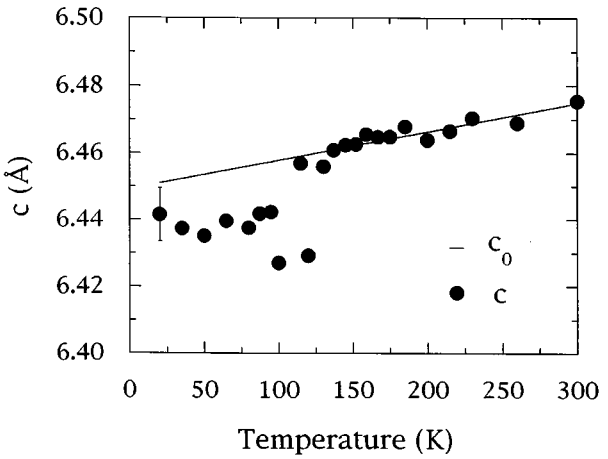

(*b*)

Figure 3. The temperature dependence of the lattice parameters of TMMC through the hexagonal $\leftrightarrow$ monoclinic phase transition. The solid lines correspond to a_0 and c_0 determined by linear least-squares fits of the experimental points in the hexagonal phase (see text).

For the sake of homogeneity, $\Delta\Phi(\eta)$ is expressed in a real form equivalent to the complex form previously adopted [13, 22, 23]:

$$\Delta\Phi(\eta) = \alpha_1(T)(\eta_1^2 + \eta_2^2) + 2\beta_1(\eta_1^3 - 3\eta_1\eta_2^2) + 2\beta_1'(\eta_2^3 - 3\eta_1^2\eta_2) + \gamma_1(\eta_1^2 + \eta_2^2)^2 + \cdots \quad (2)$$

where $\alpha_1(T) = \alpha_1^0(T - T_0)$. Note the presence of two cubic invariants that make the phase transition in η necessarily first order.

The elastic energy has the classical form:

$$\Delta\Phi(e) = \frac{1}{2}\sum_{i,j=1}^{6} C_{ij}^0 e_i e_j \quad (3)$$

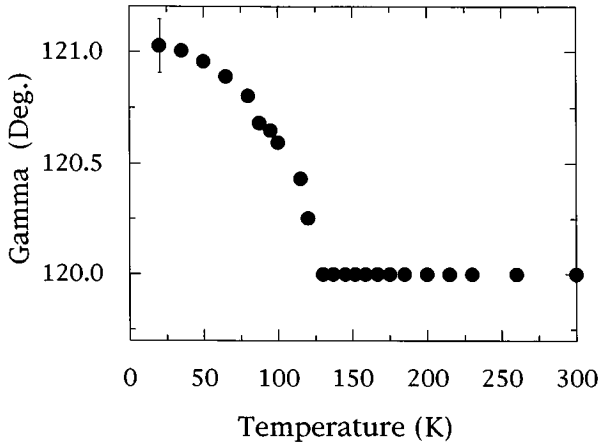

Figure 3. (Continued)

where the C^0_{ij} are the 'bare' elastic constants (in the hexagonal system $(C^0_{11}-C^0_{12})/2 = C^0_{66}$), and the e_i, e_j are the strain tensor components (Voigt notation).

$$\Delta\Phi(\eta, e) = a[\eta_1(e_1 - e_2) + \eta_2 e_6] + b[\eta_2(e_1 - e_2) - \eta_1 e_6] + d_1(e_1 + e_2)(\eta_1^2 + \eta_2^2) + d_2 e_3(\eta_1^2 + \eta_2^2) + \cdots \quad (4)$$

$$\Delta\Phi(\xi) = \alpha_2[\xi_1^2 + \xi_2^2 + \xi_3^2] + \gamma_2[\xi_1^4 + \xi_2^4 + \xi_3^4] + \delta_2[\xi_1^2\xi_2^2 + \xi_1^2\xi_3^2 + \xi_2^2\xi_3^2] + \cdots. \quad (5)$$

ξ_1, ξ_2 and ξ_3 are the three components of the OP ξ, corresponding respectively to the three arms in the star of the wavevector at point M ($0\ \frac{1}{2}\ 0$, $\frac{1}{2}\ \frac{1}{2}\ 0$, $\frac{1}{2}\ 0\ 0$).

$$\Delta\Phi(\eta, \xi) = C_1[(2\xi_1^2 - \xi_2^2 - \xi_3^2)\eta_1 + \sqrt{3}(\xi_2^2 - \xi_3^2)\eta_2] + C_2[\sqrt{3}(\xi_2^2 - \xi_3^2)\eta_1 - (2\xi_1^2 - \xi_2^2 - \xi_3^2)\eta_2]. \quad (6)$$

For convenience, the OP η and the coupling constants a and b are expressed in terms of polar coordinates, i.e.

$$\begin{cases} \eta_1 = \eta\cos\varphi \\ \eta_2 = \eta\sin\varphi \end{cases} \qquad \begin{cases} a = \Lambda\cos\psi \\ b = \Lambda\sin\psi. \end{cases} \quad (7)$$

The monoclinic phase II, $P2_1/b$ ($Z = 4$), corresponds to solutions such that [13]

$$\xi_1 = \xi \neq 0 \qquad \xi_2 = \xi_3 = 0 \quad (8)$$

since only one point in the star of M (e.g. $0\ \frac{1}{2}\ 0$) is replaced at the zone centre in this phase. Then, using relations (1)–(8) and the minimization equations $\partial\Delta\Phi(\eta, e, \xi)/\partial e_i = 0$ ($i = 1$–6), the 'effective' free energy is

$$\widetilde{\Delta\Phi}(\eta, \varphi, \xi) = \alpha_1^0(T - T_1)\eta^2 + 2(\beta_1\cos 3\varphi - \beta_1'\sin 3\varphi)\eta^3 + \gamma_1'\eta^4 + \alpha_2\xi^2 + \gamma_2\xi^4 + 2(C_1\cos\varphi - C_2\sin\varphi)\eta\xi^2 \quad (9)$$

where

$$T_1 = T_0 + \Lambda^2/2\alpha_1^0 C_{66}^0 \quad (10)$$

and

$$\gamma_1' = \gamma_1 - [2d_1^2 C_{33}^0 + d_2^2(C_{11}^0 + C_{12}^0) - 4d_1 d_2 C^0 13]/2[C_{33}^0(C_{11}^0 + C_{12}^0) - 2(C_{13}^0)^2]. \quad (11)$$

T_1 is the extrapolated temperature related to the cancellation of the elastic constant C_{66} when the transition temperature is approached from above. A fit of the experimental data gave $T_1 = 74$ K [12, 13].

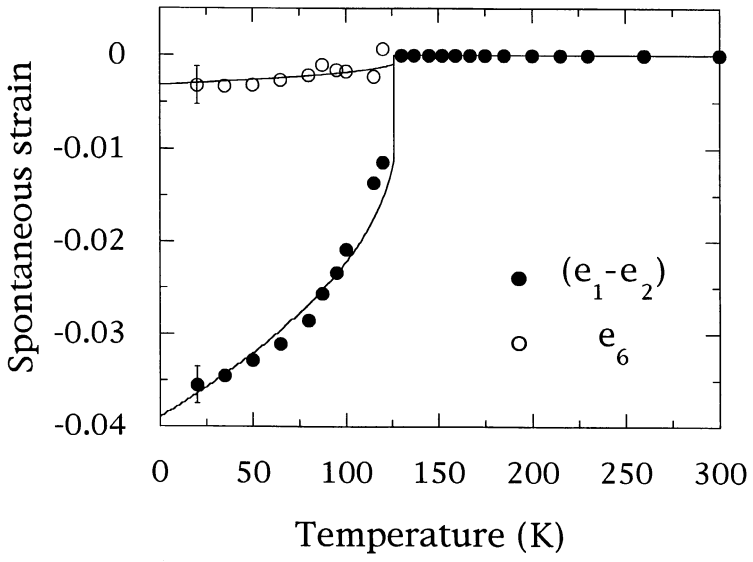

Figure 4. The temperature dependences of the strain tensor components $(e_1 - e_2)$ and e_6 of TMMC through the hexagonal↔monoclinic phase transition. The solid lines are the best fits to the data derived from relations (16), (17) and (27) (see the text).

The solutions for the potential (9), namely phase I $P6_3/m$ with $Z = 2$ ($\eta = \xi = 0$), phase III $P2_1/m$ with $Z = 2$ ($\eta \neq 0, \xi = 0$) and phase II $P2_1/b$ with $Z = 4$ ($\eta \neq 0, \xi \neq 0$), are determined by minimization, so the three following simultaneous equations must be fulfilled:

$$\partial\widetilde{\Delta\Phi}/\partial\eta = \alpha_1^0(T - T_1)\eta + 3(\beta_1 \cos 3\phi - \beta_1' \sin 3\phi)\eta^2 + 2\gamma_1'\eta^3 + (C_1 \cos\phi - C_2 \sin\phi)\xi^2 = 0 \quad (12)$$

$$\partial\widetilde{\Delta\Phi}/\partial\xi = \xi[\alpha_2 + 2\gamma_2\xi^2 + 2\eta(C_1 \cos\phi - C_2 \sin\phi)] = 0 \quad (13)$$

$$\partial\widetilde{\Delta\Phi}/\partial\phi = \eta[3(\beta_1 \sin 3\phi + \beta_1' \cos 3\phi)\eta^2 + (C_1 \sin\phi + C_2 \cos\phi)\xi^2] = 0. \quad (14)$$

It should be pointed out that there is no symmetry constraint on the direction taken by the degenerate OP η (E_{2g} symmetry) in the (η_1, η_2) plane and therefore the possibility of a temperature dependence of ϕ in the low-temperature phases arises [19]. However, as long as η contains solely pseudo-spin coordinates derived from the six-site Frenkel model, it can be shown [21] that conditions on ϕ must be enforced in order to achieve a perfect ordered state at low temperature, namely

$$\phi = k2\pi/3 \qquad (k \text{ integer modulo } 3). \quad (15)$$

For convenience, we choose $\phi = 0$, knowing that equivalent solutions (twin domains) are obtained with $k = 1$ or 2. Then, relation (14) implies $\beta_1' = 0$ and $C_2 = 0$. It follows that the spontaneous strains in the monoclinic phases II and III are given by

$$(e_1 - e_2) = -(\Lambda/C_{66}^0)\eta \cos\psi \quad (16)$$

$$e_6 = (\Lambda/C_{66}^0)\eta \sin\psi. \quad (17)$$

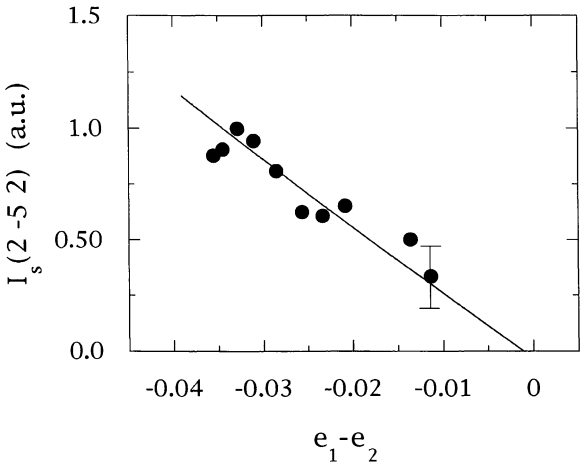

Figure 5. Intensity of the superstructure reflection (2 $\bar{5}$ 2) of TMMC observed in the monoclinic phase at different temperatures as a function of the spontaneous strain component ($e_1 - e_2$). Dots are the experimental points and the solid line is the best fit to the data according to the relation (30) (see the text).

In phase III ($\eta \neq 0, \xi = 0$), the spontaneous value of the order parameter is

$$\eta_{III} = (3\eta_c/4)[1 + \sqrt{1 - 8(T - T_1)/9(T_{III} - T_1)}] \tag{18}$$

where T_{III} is the transition temperature from phase I to phase III:

$$T_{III} = T_1 + \beta_1^2/\alpha_1^0\gamma_1' \tag{19}$$

and η_c is the jump value of η at T_{III} (first-order phase transition);

$$\eta_c = -\beta_1/\gamma_1'. \tag{20}$$

In phase II ($\eta \neq 0, \xi \neq 0$), ξ is obtained from relation (13):

$$\xi^2 = -(\alpha_2 + 2C_1\eta)/2\gamma_2. \tag{21}$$

Since α_2 and γ_2 must be positive to stabilize the effective potential (9) in the hexagonal phase, relation (21) implies the 'triggering' conditions for the occurrence of the actual first-order I $\leftrightarrow$ II phase transition:

$$C_1 > 0 \Rightarrow \eta_c < -\alpha_2/2|C_1| < 0 \tag{22}$$

$$C_1 < 0 \Rightarrow \eta_c > \alpha_2/2|C_1| > 0. \tag{23}$$

Finally, putting (21) back into (9), with $\beta_1' = C_2 = 0$, yields

$$\widetilde{\Delta\Phi(\eta)} = -\alpha_2^2/4\gamma_2 - (\alpha_2 C_1/\gamma_2)\eta + [\alpha_1^0(T - T_1) - C_1^2/\gamma_2]\eta^2 + 2\beta_1\eta^3 + \gamma_1'\eta^4 \tag{24}$$

so η_{II}, the equilibrium value of η in phase II, is given by one of the roots of the cubic equation

$$\partial\widetilde{\Delta\Phi(\eta)}/\partial\eta = -\alpha_2 C_1/\gamma_2 + 2[\alpha_1^0(T - T_1) - C_1^2/\gamma_2]\eta + 6\beta_1\eta^2 + 4\gamma_1'\eta^3 = 0. \tag{25}$$

Obviously, the form of η_{II} corresponding to the minimum of (24) cannot be conveniently expressed algebraically.

4.3. Analysis of the experimental data

First, the data of figure 4 were fitted with the help of relations (16), (17) and (25). Clearly, for such a purpose, the experimental points corresponding to (e_1-e_2) are much better suited than those corresponding to e_6, because of the large amplitude observed in the thermal evolution of $(e_1 - e_2)$ compared to that of e_6. As mentioned just above, analytical solutions of (25) cannot be conveniently handled, so we have solved this equation numerically and fitted the results to the data points by the least-squares method. Of course, the selected root, η_{II}, is the one corresponding to the true minimum of (24). The characteristic temperature T_1 was fixed to the value $T_1 = 74$ K previously determined [12, 13] and, in the first attempts, α_2 was chosen constant. Thus ξ is a secondary OP entirely 'triggered' by η [24]. This procedure provides us with acceptable solutions for temperatures up to $T \approx 120$ K; however in the range of $T_c = 126$ K $< T <$ 120 K, a change in the true minimum of (24), unavoidably occurs, thus leading to an undesirable change in the sign of $(e_1 - e_2)$. In order to avoid this intricacy, we have considered the general case of two coupled order parameters, where ξ acts as a full OP with its own temperature dependence, so we put $\alpha_2 = \alpha_2^0(T - T_2)$ with $\alpha_2^0 > 0$. Of course, in order to ensure the stability of the hexagonal phase, one should have $T_2 < T_c = 126$ K. By this means, we succeeded in fitting $(e_1 - e_2)$ in the whole range of stability of phase II.

In practice, with $\eta = R(e_1-e_2)$, $R = -C_{66}^0/(\Lambda \cos\psi)$ (see relation (16)), $(e_1-e_2) < 0$ (figure 4), we choose $R > 0$. This implies $\eta < 0$, $\beta_1 > 0$ and $C_1 > 0$; note that an equivalent choice with $R < 0$, $\eta > 0$, $\beta_1 < 0$ and $C_1 < 0$ could be made as well (see relations (20)–(23)). Then (25) is written in the form

$$-(T - T_2) + RA[(T - T_1) - \delta](e_1 - e_2) + R^2B(e_1 - e_2)^2 + R^3C(e_1 - e_2)^3 = 0 \qquad (26)$$

where

$$\begin{aligned} A &= 2\alpha_1^0\gamma_2/\alpha_2^0C_1 \\ \delta &= C_1^2/\alpha_1^0\gamma_2 \\ B &= 6\beta_1\gamma_2/\alpha_2^0C_1 \\ C &= 4\gamma_1'\gamma_2/\alpha_2^0C_1 \\ T_1 &= 74 \text{ K (fixed).} \end{aligned} \qquad (27)$$

So, it turns out that there are five independent adjustable parameters for ten data points. The best fit for the temperature dependence of $(e_1 - e_2)$ is shown in figure 4; the phenomenological coefficients take the following values:

$$\begin{aligned} RA &= 2550 \\ \delta &= 46.5 \text{ K} \\ R^2B &= 4.40 \times 10^6 \\ R^3C &= 2.91 \times 10^8 \\ T_2 &= -11.3 \text{ K.} \end{aligned} \qquad (28)$$

The agreement with the experimental data is quite satisfactory. The thermal evolution of e_6 has also been fitted by using the same set of coefficients as given in (28), with only one adjustable scale factor $R' = -\tan\psi$ (see relations (16) and (17)). Though the general trend of the variation of e_6 with temperature is well reproduced ($R' = 81 \times 10^{-3}$) (figure 4), this is not a very convincing piece of information, in consideration of the rather bad accuracy of the e_6 experimental values.

A more appropriate test for the model validity is provided by the temperature evolution of the superstructure reflection intensity I_s $(2\ \bar{5}\ 2)$. Let us define [19]

$$I_s = \lambda\xi^2. \tag{29}$$

Then, from relations (16), (21), (27) and (29)

$$I_s = (\lambda\alpha_2^0/2\gamma_2)[(T - T_2) + RA\delta(e_1 - e_2)] \tag{30}$$

where the adjustable proportionality factor is $\lambda\alpha_2^0/2\gamma_2$, all other contributing coefficients being strained according to (28). The result of the fit ($\lambda\alpha_2^0/2\gamma_2 = -2.81 \times 10^{-4}$) is reported in figure 5: the agreement is quite satisfactory.

Besides, from relations (24)–(28) the following numerical form can be deduced for the 'effective' potential:

$$\begin{aligned}\widetilde{\Delta\Phi} = P\{&(T + 11.3)[-4.8 \times 10^{-6}(T + 11.3) - (e_1 - e_2) + 1123(T - 120.4)(e_1 - e_2)] \\ &+1.46 \times 10^6(e_1 - e_2)^3 + 7.27 \times 10^7(e_1 - e_2)^4]\}\end{aligned} \tag{31}$$

where $P = R\alpha_2^0 C_1/\gamma_2$ is a constant. Plots of (31) at different temperatures are reported in figure 6. From (31), the transition temperature is determined at $T_c = 126.5 \pm 0.3$ K, in excellent agreement with previously reported values [2, 3, 7, 22, 25]. As a matter of fact, at this temperature, the fitted equilibrium spontaneous value of $(e_1 - e_2)$ abruptly changes (first-order transition) from -10.07×10^{-3} (monoclinic phase) to zero (hexagonal phase). Also, the 'triggering' condition (22) is fulfilled:

$$\eta_c = -\beta_1/\gamma_1' = -10.07 \times 10^{-3}R \ll \alpha_2^0(T_c - T_2)/2C_1 = -1.32 \times 10^{-3}R \ll 0$$

as it should be for the occurrence of the I $\leftrightarrow$ II phase transition.

Finally, it is worth noting that Levola and Kleemann [22] have interpreted the I $\leftrightarrow$ II transition of TMMC by using a Landau free energy expansion of the form

$$\Delta\Phi = \Delta\Phi(\eta) + \Delta\Phi(e) + \Delta\Phi(\eta, e)$$

which obviously cannot account for the doubling of the unit cell in phase II, because of the absence of the OP ξ and of coupling terms between η and ξ (see relations (1)–(6)). In fact, as stressed in subsection 4.2, this potential merely describes the I $\leftrightarrow$ II phase transition ($\eta \neq 0, \xi = 0$). Nevertheless, the authors of [22] fitted their (a, b) birefringence data with relation (18) and, in a narrow temperature range below T_c, they found T_c $(T_{III}) = 126.0$ K and $T_1 = 119.8$ K [22] whereas, as already mentioned, the value $T_1 = 74$ K was determined from ultrasonic measurements [12, 13]. When comparing relation (24) to (31), it now appears that the terms $-\alpha_2^2/4\gamma_2 - (\alpha_2 C_1/\gamma_2)\eta$ are always small compared to the third- and fourth-order terms. Thus, neglecting these small terms in (24), an approximate (overestimated) value of η_{II} is given by [13, 24]

$$\eta_{II} = (3\eta_c/4)[1 + \sqrt{1 - 8(T - T_1')/9(T_{II}^+ - T_1')}] \tag{32}$$

where

$$T_1' = T_1 + C_1^2/\alpha_1^0\gamma_2 \tag{33}$$

and

$$T_{II}^+ = T_1' + \beta_1^2/\alpha_1^0\gamma_1'. \tag{34}$$

T_{II}^+ is the appropriate transition temperature from phase I to phase II. Relation (32) is now of the same algebraic form as (18), but the characteristic temperatures T_{II}^+ and T_1' are renormalized ones, owing to the existence of the coupling terms between η and ξ. Hence, it turns out that the temperature T_1, as determined by Levola and Kleemann [22], was in fact

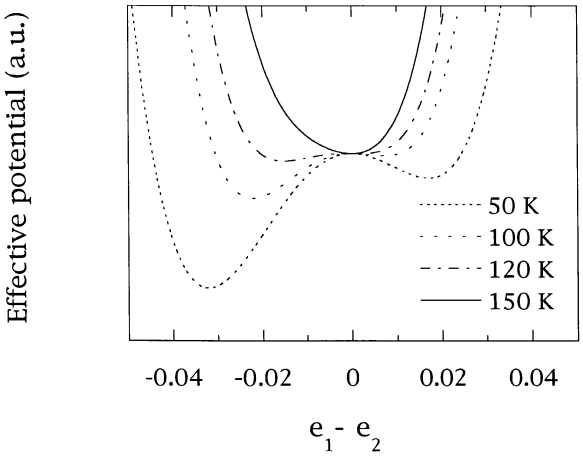

Figure 6. Plots of the 'effective' potential of TMMC at different temperatures through the hexagonal↔monoclinic phase transition, according to relation (31) (see the text).

T_1' given in (33). Using the parameters obtained from (31), i.e. $T_c \approx T_{II}^+ = 126.5$ K and $T_1' = T_1 + \delta = 120.5$ K, we verified by simple numerical simulation that the approximate relation (32) is quite able to reproduce the thermal behaviour of $(e_1 - e_2)$. Thus, the results of (a, b) birefringence [22] are in a good agreement with ours (119.5 K compared to 120.5 K for T_1' and 126.0 K compared to 126.5 K for T_c) and the apparent discrepancy between ultrasonic and birefringence measurements is now removed.

It should be mentioned however that relation (32) corresponds to a situation where α_2 is strictly equal to zero; in fact this condition represents a borderline case since it means that we are exactly at the limit of stability of the hexagonal phase I. Nevertheless, our results strongly suggest that the parameter α_2 remains small with respect to the other coefficients in (21) and (24). In other words, this leads to a rather 'flat' effective potential in the ξ direction, and consequently the existence of large fluctuations of the OP ξ can be expected. As a matter of fact, diffuse x-ray diffraction measurements performed with TMMC [9] have shown the presence of translational disorder of the octahedra chains along the hexagonal axis, related to the TA(M) mode.

5. Conclusion

A systematic investigation of TMMC as a function of temperature by means of x-ray diffraction has been performed. These new data have been confronted with the Landau free energy potential, including two coupled order parameters, previously proposed to account for the behaviour of the C_{66} elastic constant [13]. The thermal evolution of the spontaneous strain components in the monoclinic phase, $(e_1 - e_2)$ and e_6 related to the zone-centre order parameter η, as well as the intensity of superstructure reflections, related to the zone-boundary order parameter ξ responsible for unit-cell doubling at the phase transition, are satisfactorily described with this potential. Besides, (a, b) birefringence measurements [22] also comply with this model. Thus the veracity of the mechanism according to which the zone-centre order parameter 'triggers' the zone-boundary one appears to be more thermally established.

References

[1] Morosin B and Graeber E J 1967 *Acta Crystallogr.* **23** 766
[2] Peercy P S, Morosin B and Samara G A 1973 *Phys. Rev.* B **8** 3378
[3] Hutchings M T, Shirane G, Birgeneau R J and Holt S L 1972 *Phys. Rev.* B **5** 1999
[4] Magnum B W and Utton D B 1972 *Phys. Rev.* B **6** 2790
[5] Mlik Y, Daoud A and Couzi M 1979 *Phys. Status Solidi* a **52** 175
[6] Jewess M 1982 *Acta Crystallogr.* B **38** 1418
[7] Hutchings M T, Pauley G S and Stirling W G 1983 *J. Phys. C: Solid State Phys.* **16** 115
[8] Couzi M and Mlik Y 1986 *J. Raman Spectrosc.* **17** 117
[9] Braud M N, Couzi M, Chanh N B, Courseille C, Gallois B, Hauw C and Meresse A 1990 *J. Phys.: Condens. Matter* **2** 8209
[10] Rodriguez V, Aguirre-Zamalloa G, Couzi M and Roisnel T 1996 *J. Phys.: Condens. Matter* **8** 969
[11] Bradley C J and Cracknell A P 1972 *The Mathematical Theory of Symmetry in Solids* (Oxford: Clarendon)
[12] Braud M N, Couzi M, Chanh N B and Gomez-Cuevas A 1990 *J. Phys.: Condens. Matter* **2** 8229
[13] Braud M N, Couzi M and Chanh N B 1990 *J. Phys.: Condens. Matter* **2** 8243
[14] Samara G A, Peercy P S and Morosin B 1973 *Solid State Commun.* **13** 1525
[15] Fertey P and Sayetat F 1996 *J. Appl. Crystallogr.* at press
[16] Rodriguez-Carvajal J 1996 *J. Appl. Crystallogr.* submitted
Rodriguez-Carvajal J 1990 *Abstract Satellite Meeting on Powder Diffraction 15th Congr. Int. Union Crystallogr. (Toulouse, 1990)* p 127
[17] Salje E K H 1990 *Phase Transitions in Ferroelastic and Co-elastic Crystals* (Cambridge: Cambridge University Press)
[18] Schlenker J L, Gibbs G V and Boisen M B Jr 1978 *Acta Crystallogr.* A **34** 52
[19] Dorner B, Axe J D and Shirane G 1972 *Phys. Rev.* B **6** 1950
[20] Rodriguez V, Guillaume F and Couzi M 1996 *J. Phys. Chem.* at press
[21] Aguirre-Zamalloa G, Igartua J M, Couzi M and Lopez-Echarri A 1994 *J. Phyique* I **4** 1237
[22] Levola T and Kleemann W 1985 *Phys. Rev.* B **32** 4697
[23] Levola T and Laiho J 1986 *J. Phys. C: Solid State Phys.* **19** 6931
[24] Tolédano J C 1979 *Phys. Rev.* B **20** 1147
[25] Dunn A G, Jewess M, Staveley L A K and Worswick R D 1983 *J. Chem. Thermodynam.* **15** 351